

Three dimensional torus breakdown and chaos with two zero Lyapunov exponents in coupled radio-physical generators

Nataliya V. Stankevich

Laboratory of Topology methods in dynamics
National Research University High School of Economics
Nizhny Novgorod, Russia, 603155
Department of Radio-electronics and telecommunications
Yuri Gagarin State Technical University of Saratov
Saratov, Russia, 410054
Department of applied cybernetics
St. Petersburg State University
Saint-Peterburg, Russia, 198504
Email: stankevichnv@mail.ru

Natalya A. Shchegoleva

Department of Radio-electronics and telecommunications
Yuri Gagarin State Technical University of Saratov
Saratov, Russia, 410054
Email: migunovanatasha@mail.ru

Igor R. Sataev

Laboratory of theoretical nonlinear dynamics
Saratov Branch, Kotel'nikov's Institute of Radio-Engineering and Electronics of RAS
Saratov, Russia, 410019
Email: sataevir@gmail.com

Alexander P. Kuznetsov

Laboratory of theoretical nonlinear dynamics
Saratov Branch, Kotel'nikov's Institute of Radio-Engineering and Electronics of RAS
Saratov, Russia, 410019
Email: apkuz@rambler.ru

ABSTRACT

Using an example a system of two coupled generators of quasiperiodic oscillations,

we study the occurrence of chaotic dynamics with one positive, two zero and several negative Lyapunov exponents. It is shown that such dynamic arises as a result of a sequence of bifurcations of two-frequency torus doubling and involve saddle tori occurring at their doublings. This transition is associated with typical structure of parameter plane, like cross-road area and shrimp-shaped structures, based on the two-frequency quasiperiodic dynamics. Using double Poincaré section we have shown destruction of three-frequency torus.

Keywords: dynamical system, multi-frequency quasiperiodic oscillations, torus-doubling bifurcation, chaos, Lyapunov exponents

INTRODUCTION

The dynamics of ensembles of interacting oscillators is very rich and diverse. Interaction in ensembles initiates various phenomena such as: synchronization [1], [2], [3], clustering [4–6], chimeras [7–10], nonlinear resonance [11, 12] etc. Quasiperiodic oscillations are typical for interacting oscillators. In the minimal ensemble when only two self-oscillating systems interact, the simplest quasiperiodic oscillations arise, characterized by two incommensurable frequencies. Traditionally, there are two strategies for increasing the complexity of the type of quasiperiodic oscillations: (i) increasing the number of interacting elements in the ensemble; (ii) increasing the complexity of the dynamics of the base element. In both cases, it is possible to change the system in such a way that quasiperiodic oscillations with a different number of incommensurate frequency components can occur [13], [14].

An interesting and not fully studied issue is the destruction of multi-frequency quasiperiodic oscillations and the emergence of chaos [15–20]. These problem have been studied for quite a long time, for example, in this context we can talk about the scenario of turbulence in accordance with the Landau-Hopf scenario [21–23]. Destroying of torus can lead to hyperchaos via secondary Neimark-Sacker bifurcation [24–26]. But these issues are not fully explored.

The main indicator that can unambiguously distinguish and classify multi-frequency quasiperiodic oscillations is the spectrum of Lyapunov exponents [27]. When multi-frequency quasiperiodic

oscillations are destroyed, situations may arise when in the spectrum, in addition to the positive Lyapunov exponent, indicating the chaotic behavior of the observed dynamics, several zero exponents can be present [15, 16, 19, 28, 29]. A recent work [29] showed the possibility of such a chaotic behavior in a system of two coupled generators of quasiperiodic oscillations. In the frame of this work, we will consider in detail the features of chaos occurrence with an additional zero Lyapunov exponent via the destruction of the three-frequency and two-frequency quasiperiodic oscillations using the example of this system.

The work is structured as follows. In Sect. 2, we describe the object of study, the model of coupled generators of quasiperiodic oscillations, describe the structure of the parameter plane and localize the domains where three dimensional torus is destroyed and the chaos forms with one positive and two zero Lyapunov exponents. In Sect. 3, we present a detailed description of the structure of the parameter plane near the domain where chaotic oscillations with an additional zero Lyapunov exponent are observed. In Sect. 4, we discuss in detail the transition from two-frequency torus to chaos with an additional zero Lyapunov exponent via a cascade of bifurcations of torus doubling.

2. OBJECT OF STUDY: MODEL OF COUPLED GENERATORS. STRUCTURE OF THE PARAMETER PLANE, ARNOLD RESONANCE WEB

A detailed study of the dynamics of two coupled generators of quasiperiodic oscillations was presented in [29, 30]. The mathematical model, which was considered in [29, 30], can be written as follows:

$$\begin{aligned}\ddot{x}_1 - (\lambda_1 + z_1 + x_1^2 - \beta x_1^4)\dot{x}_1 + \omega_{01}^2 x_1 + M_C(\dot{x}_1 - \dot{x}_2) &= 0, \\ \dot{z}_1 &= b(\varepsilon - z_1) - k\dot{x}_1^2, \\ \ddot{x}_2 - (\lambda_2 + z_2 + x_2^2 - \beta x_2^4)\dot{x}_2 + \omega_{02}^2 x_2 + M_C(\dot{x}_2 - \dot{x}_1) &= 0, \\ \dot{z}_2 &= b(\varepsilon - z_2) - k\dot{x}_2^2,\end{aligned}\tag{1}$$

Here $x_1, \dot{x}_1 = y_1, z_1$ are the dynamical variables describing the first generator, $x_2, \dot{x}_2 = y_2, z_2$ are the dynamical variables of the second generator, M_C is the coefficient of dissipative coupling strength. Frequencies of generators are determined by the parameters ω_{01}, ω_{02} , which have the next ratio:

$$\omega_{01} = \omega_0, \omega_{02} = \omega_0 + \Delta \quad (2)$$

Δ is the frequency detuning between the generators.

The model of single oscillator described by three first-order differential equations at $M_C = 0$ was proposed in [31], where the system parameters are described. The single autonomous oscillator can undergo the Andronov-Hopf and Neimark-Sacker bifurcations with variation of parameters, as a result of which a limit cycle occurs from a stable equilibrium point, and then a two-frequency torus arises from limit cycle. This transformation can be observed by varying the parameters λ and ε , which determine the condition for the loss of stability of the equilibrium state in the system by the following equation: $\lambda = -\varepsilon$. One of the frequencies of the autonomous generator is controlled by the parameter ω_0 .

In Fig. 1 a chart of Lyapunov exponents and the main bifurcation lines are presented for single oscillator in the parameter plane (ω_0, λ) for the values of remaining other parameters:

$$\beta = 1/25, b = 1, \varepsilon = 4, k = 0.02. \quad (3)$$

The chart of Lyapunov exponents was constructed as follows: the parameter plane is scanned using some small steps over parameters ω_0 and λ and at each point of the scan the full spectrum of Lyapunov exponents was calculated using the Benettin algorithm and Gram-Schmidt orthogonalization [32]. Depending on the values of the exponents, the point on the parameter plane was painted in one color or another, in accordance with the palette shown in Fig. 1 and Table 1. Bifurcation lines were obtained using the XPPAUT application software package [33]. In Fig. 1,

the Andronov-Hopf bifurcation line corresponding to $\lambda = -4$ is marked in blue, and the Neimark-Sacker bifurcation line is shown in green. For postcritical values of the parameter λ , when the equilibrium is unstable, with a variation of the parameter ω_0 , a transition from periodic self-oscillations to quasiperiodic oscillations through the Neimark-Sacker bifurcation is observed. However, the quasiperiodic region in the parameter space is limited, and with a further increase in the parameter ω_0 , the system again goes over to periodic self-oscillations via the inverse Neimark-Sacker bifurcation.

The coupled oscillator system (1) at $M_C \neq 0$ is characterized by four independent frequencies, which are determined by the parameters of each subsystem. We consider the both oscillators identical in all parameters except the frequency parameter ω_0 , which will be changed in the second oscillator using the frequency detuning Δ . The parameters are fixed in accordance with (3) and $\lambda = 1.4$. Thus, the parameters of the first oscillator remain fixed and correspond to stable two-frequency quasiperiodic oscillations. The second oscillator, when varying the Δ parameter, demonstrates the transition from quasiperiodic to periodic oscillations through the inverse Neimark-Sacker bifurcation at $\omega_{02} \approx 8.3$. The parameter λ in the model of coupled generators plays the role of dissipation, and it is additive term to the dissipative coupling, thereafter, in coupled generators, changing the parameter of coupling, we effectively change the parameter λ of an individual subsystem, $\lambda_{eff} = \lambda - M_C$.

A detailed description of the synchronization picture for model (1) was presented in [29, 30]. Here we shortly describe main results, which will be necessary for further analysis. It was shown that for small values of the coupling strength and frequency detuning parameters, phase synchronization of quasiperiodic oscillations is observed and on the parameter plane there is a tongue of phase synchronization. Outside of this tongue the quasiperiodic oscillations with four and three incommensurable frequencies with embedded tongues of two-frequency quasiperiodicity corresponding to partial phase synchronization on subharmonics were observed. For larger coupling strength, phase synchronization with an increase in the frequency detuning is replaced by the complete synchronization mode and then the oscillation death occurred. With an increase in the non-identity of the oscillators, a regime of the so-called broadband quasiperiodicity arises [29],

which corresponds to the suppression of the dynamics of one subsystem by the other and may correspond to partial synchronization via the suppression of intrinsic dynamics, we will describe this mode in more detail below. The intersection of the partial synchronization bands forms the so-called Arnold resonance web [34–36], the destruction of which leads to the appearance of chaotic dynamics. In the frame of this work, we turn to a detailed study of chaotic attractors arising in this system during the destruction of the Arnold resonance web and characterized by one positive, two zero and three negative Lyapunov exponents.

For understanding and analyzing the scenario of formation of the complex behavior in the presented model we need a special tool which would allow us to distinguish and analyze quasiperiodic and chaotic oscillations. Unfortunately, at the present moment there are no adequate methods for analyzing quasiperiodic bifurcations, developed up to a comparable degree as those for bifurcations of periodic regimes. In the present paper we use the following approaches: (i) analysis of the full spectrum of Lyapunov exponents, method of charts of Lyapunov exponents; (ii) rigorous bifurcation analysis of quasiperiodic oscillations based on consideration of behavior of the Lyapunov exponents near a bifurcation point. The first approach was mentioned and described above. In accordance with a rigorous bifurcation analysis of tori suggested in [37], analyzing behavior of the Lyapunov exponents near a bifurcation point one can distinguish three quasiperiodic bifurcations. *Quasiperiodic Hopf bifurcation*: before the bifurcation point, two maximal negative Lyapunov exponents coincide: $\Lambda_n = \Lambda_{n+1}$. At the bifurcation point, both of them touch zero axis, then one of them vanishes: $\Lambda_n = 0$, and the other Λ_{n+1} becomes negative. *Saddle-node quasiperiodic bifurcations*: before the bifurcation point, two negative Lyapunov exponents after zero are not the same, Λ_n and Λ_{n+1} . At the bifurcation point, one of them vanishes: $\Lambda_n = 0$, and the other Λ_{n+1} remains negative, and does not touch zero. *Period-doubling of torus*: before the bifurcation point, two negative Lyapunov exponents after zero are not the same, Λ_n and Λ_{n+1} . At the bifurcation point, one of them touches zero: $\Lambda_n = 0$, and the other Λ_{n+1} remains negative. In our numerical simulations we use the 4th order Runge-Kutta method with step size 10^{-2} . When calculating Lyapunov exponents the length of averaging interval was equal 70000 time units.

Figure 2 shows a chart of Lyapunov exponents on the parameter plane of the frequency detun-

ing Δ and the coupling strength coefficient M_C (Fig. 2a), its zoomed fragment for small values of the coupling parameter (Fig. 2b) and its zoomed fragment, where a transition from four-frequency to three-frequency quasiperiodic dynamics is observed (Fig. 2c). System (1) is characterized by six Lyapunov exponents, depending on which six types of dynamic behavior can be classified: stable equilibrium point (oscillation death), periodic oscillations, three types of quasiperiodic regimes, and chaotic oscillations; Fig. 2 shows the corresponding palette, Table 2 shows the according signature of the spectrum of Lyapunov exponents. In accordance with the spectrum of Lyapunov exponents, we also distinguished three types of chaotic dynamics: (i) chaos with one positive, one zero, and four negative Lyapunov exponents (gray); (ii) chaos with one positive, two zero and three negative Lyapunov exponents (black); (iii) hyperchaos with two positive, one zero and three negative Lyapunov exponents (white color). Spectra of Lyapunov exponents were calculated with a certain accuracy, and we must enter a threshold value to distinguish between zero and non-zero exponents. In our numerical experiments, when constructing charts of Lyapunov exponents, we fixed the threshold of equality of Lyapunov exponents to zero equal to 10^{-3} , i.e. if $|\Lambda_i| < 10^{-3}$, then we assume that the exponent is zero. Moreover, in the case when we observe several zero Lyapunov exponents in the spectrum (it can be both a case of quasiperiodic oscillations with different incommensurate frequencies and a case of chaos with additional zero Lyapunov exponent), they will be a little bit different, but with an increase in the calculation accuracy, they will approach to zero.

On the chart of Lyapunov exponents, the phase synchronization region is marked by *PS*, it has a form of tongue with a base at the point of zero frequency detuning and coupling strength. For a small coupling strength and not very large frequency detuning, four-frequency quasiperiodic modes T_4 are observed, inside which there are bands of three-frequency quasiperiodic modes T_3 , such transitions correspond to partial synchronization when the second generator gets into the synchronization tongues of autonomous generator. Tongues of two-frequency quasiperiodicity are also visible on the chart of coupled oscillators, but they have a certain threshold in the coupling strength. At $\Delta = \Delta_{NS} \approx 5.15$, the second autonomous subsystem crosses the Neimark-Sacker bifurcation line, which corresponds to the transition to three-frequency quasiperiodic oscillations

in a system of coupled oscillators (1). With a frequency detuning larger than Δ_{NS} , tongues of two-frequency quasiperiodicity are observed at higher harmonics, which also represent partial frequency locking, but in this case, as a result of locking, two-frequency quasiperiodic oscillations are observed.

For large values of the parameters of the frequency detuning and coupling strength, a region of oscillation death (E) is observed, which corresponds to the suppression of the intrinsic dynamics of oscillators due to strong dissipation introduced into the system by a dissipative coupling. The decrease in the coupling leads to the fact that, at $M_C = 5.4 = (1.4 - (-4))$, the equilibrium state loses stability (since $\lambda_{eff} = \lambda - M_C = -4 = -\varepsilon$ which corresponds to Andronov-Hopf bifurcation in the individual subsystem), and as a result two-frequency quasiperiodic regime occurs. This domain of two-frequency quasiperiodic regime is the so-called broadband quasiperiodicity (BQ) [29]. In [29], the features of attractors in this area are described in detail. With a further decrease in the coupling strength a three-frequency quasiperiodic regime is born as a result of quasiperiodic Hopf bifurcation. Along the line of quasiperiodic Hopf bifurcation, there is a system of two-frequency quasiperiodic tongues corresponding to partial synchronization. At further decreasing of the coupling parameter M_C , there is set of bands of two-frequency quasiperiodic regimes alternating with bands of three-frequency or chaotic oscillations in the parameter plane. The boundaries of such bands correspond to saddle-node quasiperiodic bifurcations (i.e., saddle-node bifurcations of invariant tori). Such bands of two-frequency quasiperiodic regimes form the Arnold resonance web. At the intersections of the two-frequency quasiperiodic bands, resonances of higher order (periodic regimes) are observed. In the vicinity of the intersections, a complex structure is observed, consisting of tongues of two-frequency quasiperiodic regimes.

Figure 2 c shows an enlarged fragment of the chart in the vicinity of the island of periodic oscillations. At the intersection of the regions of two-frequency quasiperiodic dynamics, complete synchronization is observed. The fragment clearly shows the intersection of the regions of two-frequency quasiperiodicity corresponding to different types of partial synchronization: phase synchronization of quasiperiodic oscillations on subharmonics (the tip of tongue of such synchronization extend from the axis of zero coupling strength) and broadband quasiperiodicity (horizontal

bands).

Figure 3 shows the two-dimensional projections of phase portraits on the dynamic variables (x , z) of each of the oscillators in the Poincaré section by the hypersurface $y_1 = 0$ for tongues of two-frequency quasiperiodic oscillations corresponding to different types of partial synchronization.

Phase portraits in Figs 3a - 3c correspond to the tongues of two-frequency tori arising on subharmonics; points on the parameter plane are depicted in Fig. 2c by green dots and letters. For a small coupling strength, a smooth invariant curve is observed in the projection onto the variables of the first generator in the Poincaré section. The invariant curve in the projection onto the variables of the second generator is different: it has the shape of a two-turn figure eight, but it is also smooth and continuous. Increasing of the coupling strength in that way that one cross the horizontal band of broadband quasiperiodicity on the parameter plane, but also stay inside the synchronization tongue which contains the complete synchronization domain, then phase portraits will retain their structure (examples in Fig. 3b, 3c). The invariant curve in the projection onto the variables of the first generator remains almost unchanged for values of frequency detuning and coupling strength corresponding to the region to the left of the domain of complete synchronization (Fig. 3b). For the parameter values corresponding to the partial synchronization area to the right from the tongue of complete synchronization, the bends of the invariant curve become sharper, and some of them transform into loops (Fig. 3c). In the projection onto the dynamic variables of the second generator, the invariant curve changes more, additional loops appear, and the figure-eight is violated.

Figs. 3d - 3f show examples of phase portraits for a broadband quasiperiodicity band. In this case an invariant curve projected onto the dynamic variables of the first generator has a fundamentally different structure: five smooth closed invariant curves are observed in the Poincaré section. Such form of invariant curve corresponds to the so-called multi-layered torus [38, 39]. In the projection onto the dynamic variables of the second generator for frequency detunings to the left from tongue of complete synchronization, the invariant curve has a rather complicated structure. For larger values of frequency detunings, directly inside the broadband quasiperiodic band, the invariant curve in the projection onto the dynamic variables of the second generator

takes the form of a figure eight, however, the number of loops which the phase trajectory makes in figure eight increases. It means that the winding number of torus is changing.

Figure 3g shows an example of a phase portrait for a two-frequency quasiperiodic tongue located between the broadband quasiperiodic band and the main tongue in subharmonics. In this case the invariant curve in the projection onto the variables of the first generator has one invariant curve, but additional loops appear in that places, where several invariant curves for wideband quasiperiodicity have place. The invariant curve in the projection onto the dynamic variables of the second generator has the shape of a figure-eight, however, the number of loops increases.

3. THREE-FREQUENCY TORUS, ITS DESTRUCTION

Figure 4a shows an zoomed fragment of the Lyapunov exponent chart, which visualizes in detail the structure of the two-frequency tori tongues set embedded into domain of three-frequency quasiperiodic oscillations. The structure of the region is similar to the classical Arnold tongues which is character for the circle map [40], but with additional incommensurable frequency. When tongues overlap, chaos emerges. The chaos has a feature: the spectrum of Lyapunov exponents contains one positive, two zero and three negative Lyapunov exponents. The tongues of two-frequency tori have developed internal structures, bifurcations of torus doubling occur inside, and the shape of the tongues looks like the "Crossroad-area structures" which is typical for the transformation of limit cycles in accordance with the Feigenbaum period-doubling scenario [42], [41].

As was mentioned above, this structure on the parameter plane is observed in the vicinity of the intersection of the synchronization tongue at higher harmonics and broadband quasiperiodicity band. Figures 3a - 3e show examples of two-dimensional projections of phase portraits in the Poincaré section for each of the regions of two-frequency quasiperiodicity, between which a set of tongues of two-frequency quasiperiodicity embedded into the three-frequency quasiperiodic regimes is observed.

Figures 4b - 4d show two-dimensional projections of phase portraits in the Poincaré section with the hypersurface $y_1 = 0$ from various tongues of two-frequency tori, green letters mark the corresponding points in Fig. 4a. Projections on the plane of the first (x_1, z_1) and second $(x_2,$

z_2) generators in this case are also very different from each other. In the central tongue the projection onto the plane of the variables of the first generator (x_1, z_1) is close to a one-turn torus (Fig. 4b): one smooth closed invariant curve without self-intersections, however, there are 5 bends corresponding to the five-turn torus, which was observed inside the region of two-frequency oscillations corresponding to broadband quasiperiodicity. In the projection onto the variables of the second oscillator (x_2, z_2) , the invariant curve has the shape of a figure of eight, consisting of 7 loops with self-intersections.

In another tongues, which are observed with an increase of the frequency detuning (moving on the parameter plane towards the domain of broadband quasiperiodicity, up and right in Fig. 4a), on the invariant curve in the projection onto the variables of the first oscillator additional loops arise in the vicinity of the invariant curves of the five-turn torus. Moreover, in the projection onto the variables of the second generator, the number of loops in the figure-eight increases in accordance with the number of additional loops around multi-turn invariant curves. Thus in Fig. 4c, 12 rotations in the figure-eight are observed, in Fig. 4d - 17 rotations. In tongues, which are observed with an decrease of the frequency detuning and approaching the partial synchronization region at higher harmonics, the invariant curve transforms in another way (Fig. 4e): the basic invariant curve is doubled in the projection onto the dynamic variables of the first oscillator, and in the projection onto the variables of the second oscillator the number of loops around the figure-eight also increases, so for the invariant curve in Fig. 4e there are 9 rotations. Thus, in this domain of the parameter plane, we see the emergence of a complex picture of the partial synchronization tongues, corresponding to two-frequency tori, on the surface of a three-frequency torus. Conventionally, for tongues of two-frequency quasiperiodicity, one can introduce winding numbers in accordance with the number of rotations of the invariant curve, which vary in different tongues of two-frequency tori.

It is well known that in the classical picture of synchronization, which can be observed, for example, in circle map, with a change in the parameters the overlapping of the synchronization tongues is possible, which lead to the destruction of quasiperiodic oscillations and emergence of chaotic attractor. The same transformations observed for our model but the base dynamical mode in our case is a three-frequency torus, the boundaries of the tongues of two-frequency quasiperi-

odicity correspond to saddle-node quasiperiodic bifurcations, as a result of which a two-frequency torus is born. When the tongues of two-frequency tori overlap, the three-frequency torus is destroyed with the formation of a chaotic attractor. Usually such a destruction of the torus is associated with a loss of smoothness of the invariant curve. For our case, such a transformation should be associated with the loss of smoothness and destruction of the three-frequency torus. In order to visualize such a transformation, we use the multi-fold Poincaré section technique [43], [44]. In order to visualize the invariant curve of a three-frequency quasiperiodic regime, it is necessary to implement a double Poincaré section. We have to note that in Poincaré section the set of points is discrete and we need to fix points inside some thin slice of phase space, in our numerical experiments we take slice in accordance with the follow condition: $(|y_1| < 0.01) \cap (|y_2| < 0.01)$. Figure 5 shows examples of projections of phase portraits in a double Poincaré section with the hypersurface $y_1 = 0, y_2 = 0$. The portraits in Figs. 5a and 5b are constructed for parameters corresponding to three-frequency quasiperiodic modes. The phase portrait in the double Poincaré section in this case has the form of a smooth invariant curve. The shape of the invariant curve in projection onto the variables of the first generator is very close to that which occurs for a two-frequency torus in a single Poincaré section, it has the form of a doubled invariant curve. Projections on the variables of the second oscillator have a more complex structure, but it is still smooth and continuous.

Figures 5c and 5d show examples of phase portraits in the double Poincaré section for destroyed three-frequency tori. In this case the invariant curve in double Poincaré section loses smoothness, and occurring chaotic attractors have some features: the spectrum of Lyapunov exponents includes an additional zero Lyapunov exponent. Table 3 presents the Lyapunov exponents for the chaotic attractors shown in Fig. 5. Double Poincaré section in the Fig. 5c demonstrates the banded structure of the arising attractor. Such attractors can be reached on the parameter plane from the tongues of two-frequency quasiperiodicity through a cascade of bifurcations of invariant curve doubling. The chaotic attractors arising in this way have the same specifics: the spectrum of Lyapunov exponents contains one positive and two zero Lyapunov exponents. In the next Section, we will consider in detail the formation of such chaotic attractor as a result of a cascade of invariant curve doubling bifurcations.

4. THE EMERGENCE OF CHAOS WITH AN ADDITIONAL ZERO LYAPUNOV EXPONENT AS A RESULT OF A CASCADE OF TORUS DOUBLING BIFURCATIONS

Figure 4a shows that there are doubling bifurcations of two-frequency tori inside the tongues of two-frequency quasiperiodicity. As a result of cascade of torus doubling bifurcations a chaos with one positive, two zero and three negative Lyapunov exponents emerges. For a more detailed analysis of the scenario of the appearance of such kind chaotic attractors, we construct a zoomed fragment of the chart of Lyapunov exponents for coupled quasiperiodic generators (1) in the chaos region.

The tongues of two-frequency quasiperiodic dynamics have an internal structure: with a change in parameters, several two-frequency torus doubling bifurcations are observed, and then a chaotic attractor is formed containing an additional zero Lyapunov exponent in the spectrum. In Fig. 6a there is a zoomed fragment of the Lyapunov exponent chart showing the internal structure of one of the two-frequency quasiperiodic tongues. The Lyapunov exponents chart also shows lines corresponding to bifurcations of doubling of the two-frequency torus, shown in blue. The structure of the tongue has characteristic features for the structure of the "crossroad area": the stability region of the two-torus is bounded by doubling lines, as well as two lines of folds forming the lower border. The lines of folds extend into the stability region of the 2-torus and converge at a point, which in catastrophe theory is called the cusp point. Inside the chaos region there are windows of two-frequency quasiperiodicity, which are called Shrimp-Shaped Domains [42, 45, 46].

Let us consider in detail the transition from a two-frequency torus to chaos using the example of projections of phase portraits in the Poincaré section. The parameter Δ was fixed: $\Delta = 5.35$, and the parameter of coupling strength gradually increased, so that torus doubling bifurcations were observed. Figs. 6b - 6e show the first three bifurcations of the cascade in the projection onto the dynamic variables of the first generator (we used this projection, since the invariant curve is clearly visible on it). The shape of the attractor is quite complex, so it is very difficult to see subsequent doublings or other transformations of the invariant curve in a full phase portrait. In order to track further changes, we construct zoomed fragments that show the structure of the attractor, in Figs. 6e, 6f and 6h, green rectangles indicate zoomed fragments. On the enlarged

fragments, one can observe clearly another five doubling of the torus (Fig. 6f - 6i). Thus, we were able to detect eight bifurcations of doubling of the two-frequency torus, i.e. birth of a 128-turn two-frequency torus.

Figures 7a - 7e show the development of a chaotic attractor using the example of projections of phase portraits in the Poincaré section at varying coupling strength. To check the chaoticity for each point the full spectrum of Lyapunov exponents was calculated, which are shown in Table 4. With an increase in the coupling parameter, the invariant curves expand, bands are formed, and the attractor becomes chaotic, while in the spectrum of Lyapunov exponents there are one positive and two zero exponents. The bands gradually expand, the space between them is filled. In this case, the points uniformly fill the attractor. When passing through the windows of two-frequency quasiperiodicity, the chaotic attractor becomes more uniform, the bands that are not filled with phase points disappear, and bands of attractor are merged.

The formation of such chaotic attractor can be explained as follows. Each bifurcation of the doubling of a torus occurs as a result of the loss of its stability. Before bifurcation, a stable torus is observed in the phase space, after it a stable torus becomes a saddle torus which has two-dimensional neutral manifold, and a new stable two-turn torus is born. As a result of the cascade of bifurcations of torus doubling, the set of saddle tori accumulate that have a two-dimensional neutral manifold. When the torus is finally destroyed, chaotic attractor absorbs saddle tori, which leads to the fact that the spectrum of Lyapunov exponents contains two zero exponents characterizing a two-dimensional neutral manifold. For the considered model, the invariant curves didn't lose smoothness, thus, we can assume that the cascade of torus doubling bifurcations is very long, if not infinite. Additionally it may be assumed at the band merging points a homoclinic bifurcation of the torus occurs in analogy with band merging mechanism for Feigenbaum period doubling scenario [47, 48], as a result of which a countable set of saddle tori is born in its vicinity, this set is also absorbed by the attractor. Fig. 7e shows an example of the eventually fully developed one-band chaotic attractor, it has a dense uniform packing. We also note that the growing of the attractor is accompanied by an increase in the largest positive Lyapunov exponent, while the two next exponents are zero, and were diagnosed with accuracy of 10^{-6} . In [49] such type of attractors

was called quasi-periodic Hénon-like.

As an additional illustration of this transition, one-parameter graphs of Lyapunov exponents can be used. Figure 8 shows the dependence of the largest three Lyapunov exponents on the coupling strength parameter for the transition from the central tongue of two-frequency quasiperiodicity to chaos with two zero Lyapunov exponents. During the transition, the torus doubling bifurcations are clearly distinguishable (DT^{11} , DT^{12} , DT^{21} , DT^{31} , DT^{32} in Fig. 8a, here the first digit of the index simply identifies the specific cascade and the second one denotes the serial number of the bifurcation in the cascade), after which the largest Lyapunov exponent Λ_1 becomes positive, and the next two Λ_2 and Λ_3 are equal zero. Such transitions on the graph we observed three times, i.e. they can be implemented for different two-frequency quasiperiodic tongues that correspond to different Shrimp-Shaped Domains.

Figures 8b - 8d show zoomed fragments of Fig. 8a on which tori with the corresponding number of doublings are signed. Thus, in a numerical experiment, we were able to observe 8 bifurcations of the doubling of the torus, after which chaos is observed in the system. A further decrease in the range of parameters leads to an increase in the numerical error in calculating the spectrum of Lyapunov exponents.

CONCLUSIONS

Thus, in the frame of this work, it was shown that in the system of two coupled generators of quasiperiodic oscillations with a small coupling strength a specific type of chaotic dynamics may arise, characterized by the presence of one positive and two zero Lyapunov exponents in the spectrum. The mechanism of occurrence of such chaotic attractor can be associated with a cascade of invariant curve doubling bifurcations. As a result of cascade the set of saddle tori with two-dimensional neutral manifold occurs. Absorption of this set by chaotic attractor lead to formation of chaotic attractor with additional zero Lyapunov exponent in the spectrum. The structure of the parameter plane was also described, where such chaotic attractors can arise. Appearance of such chaotic dynamics is associated with destruction of Arnold resonance web, and competition between different type of partial synchronization for the model with several incommensurable

frequencies. The possibility of the appearance of typical structures such as Cross-Road Area and Shrimp-Shaped Domains, but based on two-frequency quasiperiodic modes, the transformation of which leads to chaos with one positive, two zero and three negative Lyapunov exponents is shown.

ACKNOWLEDGEMENTS

The reported study was funded by Russian Foundation of Basic Research, project number 19-31-60030 (Introduction, Sects. 3, 4, Conclusion) and the grant of the President of the Russian Federation MK-31.2019.8 (Sect.2). The work of A.P.K. and I.R.S. was carried out within the framework of the state task of Kotel'nikov's IRE RAS

REFERENCES

- [1] Pikovsky, A., Kurths, J., Rosenblum, M., and Kurths, J., 2003. *Synchronization: a universal concept in nonlinear sciences*, Vol. 12. Cambridge university press.
- [2] Anishchenko, V. S., Vadivasova, T. E., and Strelkova, G. I., 2014. "Synchronization of periodic self-sustained oscillations". In *Deterministic Nonlinear Systems*. Springer, pp. 217–243.
- [3] Shilnikov, A., Shilnikov, L., and Turaev, D., 2004. "On some mathematical topics in classical synchronization.: A tutorial". *International Journal of Bifurcation and Chaos*, **14**(07), pp. 2143–2160.
- [4] Belykh, V. N., Belykh, I. V., Hasler, M., and Nevidin, K. V., 2003. "Cluster synchronization in three-dimensional lattices of diffusively coupled oscillators". *International Journal of Bifurcation and Chaos*, **13**(04), pp. 755–779.
- [5] McGraw, P. N., and Menzinger, M., 2005. "Clustering and the synchronization of oscillator networks". *Physical Review E*, **72**(1), p. 015101.
- [6] Czolczynski, K., Perlikowski, P., Stefanski, A., and Kapitaniak, T., 2009. "Clustering and synchronization of n Huygens clocks". *Physica A: Statistical Mechanics and its Applications*, **388**(24), pp. 5013–5023.
- [7] Abrams, D. M., and Strogatz, S. H., 2006. "Chimera states in a ring of nonlocally coupled

- oscillators”. *International Journal of Bifurcation and Chaos*, **16**(01), pp. 21–37.
- [8] Bordyugov, G., Pikovsky, A., and Rosenblum, M., 2010. “Self-emerging and turbulent chimeras in oscillator chains”. *Physical Review E*, **82**(3), p. 035205.
- [9] Omelchenko, I., Maistrenko, Y., Hövel, P., and Schöll, E., 2011. “Loss of coherence in dynamical networks: spatial chaos and chimera states”. *Physical review letters*, **106**(23), p. 234102.
- [10] Ashwin, P., and Burylko, O., 2015. “Weak chimeras in minimal networks of coupled phase oscillators”. *Chaos: An Interdisciplinary Journal of Nonlinear Science*, **25**(1), p. 013106.
- [11] Nayfeh, A. H., and Balachandran, B., 1989. “Modal interactions in dynamical and structural systems”. *Appl. Mech. Rev.*, **42**(11), pp. 175–201.
- [12] Balachandran, B., and Nayfeh, A., 1992. “Cyclic motions near a hopf bifurcation of a four-dimensional system”. *Nonlinear Dynamics*, **3**(1), pp. 19–39.
- [13] Emelianova, Y. P., Kuznetsov, A., Sataev, I., and Turukina, L., 2013. “Synchronization and multi-frequency oscillations in the low-dimensional chain of the self-oscillators”. *Physica D: Nonlinear Phenomena*, **244**(1), pp. 36–49.
- [14] Emelianova, Y. P., Emelyanov, V. V., and Ryskin, N. M., 2014. “Synchronization of two coupled multimode oscillators with time-delayed feedback”. *Communications in nonlinear science and numerical simulation*, **19**(10), pp. 3778–3791.
- [15] Kaneko, K., 1983. “Doubling of torus”. *Progress of theoretical physics*, **69**(6), pp. 1806–1810.
- [16] Kaneko, K., 1984. “Oscillation and doubling of torus”. *Progress of Theoretical Physics*, **72**(2), pp. 202–215.
- [17] Anishchenko, V., Safonova, M., Feudel, U., and Kurths, J., 1994. “Bifurcations and transition to chaos through three-dimensional tori”. *International Journal of Bifurcation and Chaos*, **4**(03), pp. 595–607.
- [18] Alaggio, R., and Rega, G., 2000. “Characterizing bifurcations and classes of motion in the transition to chaos through 3d-tori of a continuous experimental system in solid mechanics”. *Physica D: Nonlinear Phenomena*, **137**(1-2), pp. 70–93.
- [19] Pazó, D., Sánchez, E., and Matias, M. A., 2001. “Transition to high-dimensional chaos through quasiperiodic motion”. *International Journal of Bifurcation and Chaos*, **11**(10), pp. 2683–2688.

- [20] Anishchenko, V., and Nikolaev, S., 2005. “Generator of quasi-periodic oscillations featuring two-dimensional torus doubling bifurcations”. *Technical physics letters*, **31**(10), pp. 853–855.
- [21] Landau, L. D., 1944. “On the problem of turbulence”. In Dokl. Akad. Nauk USSR, Vol. 44, p. 311.
- [22] Hopf, E., 1948. “A mathematical example displaying features of turbulence”. *Communications on Pure and Applied Mathematics*, **1**(4), pp. 303–322.
- [23] Kuznetsov, A. P., Kuznetsov, S. P., Sataev, I. R., and Turukina, L. V., 2013. “About landau–hopf scenario in a system of coupled self-oscillators”. *Physics Letters A*, **377**(45-48), pp. 3291–3295.
- [24] Stankevich, N. V., Dvorak, A., Astakhov, V., Jaros, P., Kapitaniak, M., Perlikowski, P., and Kapitaniak, T., 2018. “Chaos and hyperchaos in coupled antiphase driven Toda oscillators”. *Regular and Chaotic Dynamics*, **23**(1), pp. 120–126.
- [25] Garashchuk, I. R., Sinelshchikov, D. I., Kazakov, A. O., and Kudryashov, N. A., 2019. “Hyperchaos and multistability in the model of two interacting microbubble contrast agents”. *Chaos: An Interdisciplinary Journal of Nonlinear Science*, **29**(6), p. 063131.
- [26] Stankevich, N., Kuznetsov, A., Popova, E., and Seleznev, E., 2019. “Chaos and hyperchaos via secondary neimark–sacker bifurcation in a model of radiophysical generator”. *Nonlinear Dynamics*, **97**(4), pp. 2355–2370.
- [27] Pikovsky, A., and Politi, A., 2016. *Lyapunov exponents: a tool to explore complex dynamics*. Cambridge University Press.
- [28] Stankevich, N., Astakhov, O., Kuznetsov, A., and Seleznev, E., 2018. “Exciting chaotic and quasi-periodic oscillations in a multicircuit oscillator with a common control scheme”. *Technical Physics Letters*, **44**(5), pp. 428–431.
- [29] Kuznetsov, A., Kuznetsov, S., Shchegoleva, N., and Stankevich, N., 2019. “Dynamics of coupled generators of quasiperiodic oscillations: Different types of synchronization and other phenomena”. *Physica D: Nonlinear Phenomena*.
- [30] Kuznetsov, A. P., and Stankevich, N. V., 2018. “Dynamics of coupled generators of quasi-periodic oscillations with equilibrium state”. *Izvestiya VUZ. Applied Nonlinear Dynamics*,

26(2), pp. 41–58.

- [31] Kuznetsov, A., Kuznetsov, S., Mosekilde, E., and Stankevich, N., 2013. “Generators of quasiperiodic oscillations with three-dimensional phase space”. *The European Physical Journal Special Topics*, **222**(10), pp. 2391–2398.
- [32] Benettin, G., Galgani, L., Giorgilli, A., and Strelcyn, J.-M., 1980. “Lyapunov characteristic exponents for smooth dynamical systems and for hamiltonian systems; a method for computing all of them. part 1: Theory”. *Meccanica*, **15**(1), pp. 9–20.
- [33] Ermentrout, B., 2002. *Simulating, analyzing, and animating dynamical systems: a guide to XPPAUT for researchers and students*, Vol. 14. Siam.
- [34] Froeschlé, C., Guzzo, M., and Lega, E., 2000. “Graphical evolution of the arnold web: from order to chaos”. *Science*, **289**(5487), pp. 2108–2110.
- [35] Broer, H., Simó, C., Vitolo, R., et al., 2008. “The hopf-saddle-node bifurcation for fixed points of 3d-diffeomorphisms: the arnol’d resonance web”. *Bulletin of the Belgian Mathematical Society-Simon Stevin*, **15**(5), pp. 769–787.
- [36] Sekikawa, M., Inaba, N., Kamiyama, K., and Aihara, K., 2014. “Three-dimensional tori and arnold tongues”. *Chaos: An Interdisciplinary Journal of Nonlinear Science*, **24**(1), p. 013137.
- [37] Vitolo, R., Broer, H., Simó, C., 2008. “Quasi-periodic bifurcations of invariant circles in low-dimensional dissipative dynamical systems”. *Regular and Chaotic Dynamics*, **16**(1-2), pp. 154-184.
- [38] Zhusubaliyev, Z. T., and Mosekilde, E., 2009. “Novel routes to chaos through torus breakdown in non-invertible maps”. *Physica D: Nonlinear Phenomena*, **238**(5), pp. 589–602.
- [39] Zhusubaliyev, Z. T., Laugesen, J. L., and Mosekilde, E., 2010. “From multi-layered resonance tori to period-doubled ergodic tori”. *Physics Letters A*, **374**(25), pp. 2534–2538.
- [40] Arnol’d, V. I., 2012. *Geometrical methods in the theory of ordinary differential equations*, Vol. 250. Springer Science & Business Media.
- [41] Carcasses, J., Mira, C., Bosch, M., Simó, C., and Tatjer, J., 1991. ““crossroad area – spring area” transition (i) parameter plane presentation”. *International Journal of Bifurcation and Chaos*, **1**(01), pp. 183–196.

- [42] Gallas, J. A., 1993. "Structure of the parameter space of the h enon map". *Physical Review Letters*, **70**(18), p. 2714.
- [43] Moon, F., and Holmes, W., 1985. "Double poincar e sections of a quasi-periodically forced, chaotic attractor". *Physics Letters A*, **111**(4), pp. 157–160.
- [44] Stankevich, N., Kuznetsov, A., Popova, E., and Seleznev, E., 2017. "Experimental diagnostics of multi-frequency quasiperiodic oscillations". *Communications in Nonlinear Science and Numerical Simulation*, **43**, pp. 200–210.
- [45] Stoop, R., Benner, P., and Uwate, Y., 2010. "Real-world existence and origins of the spiral organization of shrimp-shaped domains". *Physical review letters*, **105**(7), p. 074102.
- [46] Barrio, R., Blesa, F., Serrano, S., and Shilnikov, A., 2011. "Global organization of spiral structures in biparameter space of dissipative systems with shilnikov saddle-foci". *Physical Review E*, **84**(3), p. 035201.
- [47] Sim o, C., 1979. "On the h enon-pomeau attractor". *Journal of Statistical Physics*, **21**(4), pp. 465–494.
- [48] R ossler, O., Stewart, H., and Wiesenfeld, K., 1990. "Unfolding a chaotic bifurcation". *Proceedings of the Royal Society of London. Series A: Mathematical and Physical Sciences*, **431**(1882), pp. 371–383.
- [49] Vitolo, R., Broer, H., and Sim o, C., 2010. "Routes to chaos in the hopf-saddle-node bifurcation for fixed points of 3d-diffeomorphisms". *Nonlinearity*, **23**(8), p. 1919.

LIST OF TABLES

1	Accordance between signature of the Lyapunov exponents spectrum of observed regimes and symbols used for the charts of Lyapunov exponents for 3D system of autonomous quasiperiodic generator	24
2	Accordance between signature of the Lyapunov exponents spectrum of observed regimes and symbols used for the charts of Lyapunov exponents for 6D system of coupled generators	28
3	Signature of the spectrum of the Lyapunov exponents for attractors at transition to chaos via three-torus destruction, parameters (3) and $\lambda = 1.4, \omega_0 = 2\pi$	29
4	Signature of the spectrum of the Lyapunov exponents for attractors at transition to chaos via two-torus doubling bifurcations, parameters (3) and $\lambda = 1.4, \omega_0 = 2\pi$. . .	29

LIST OF FIGURES

- 1 Chart of Lyapunov exponents and the main bifurcation lines of autonomous generator of quasiperiodic oscillations, system (1) with parameters (3) and $M_C = 0$, $\Delta = 0$. *HB* is line of Andronov-Hopf bifurcation, *NS* is line of Neimark-Sacker bifurcation. 24

- 2 Chart of Lyapunov exponents and its enlarged fragments for the system of coupled quasiperiodic generators (1) with parameters $\beta = 1/25$, $b = 1$, $\varepsilon = 4$, $k = 0.02$, $\lambda = 1.4$, $\omega_0 = 2\pi$ 24

- 3 Two-dimensional projections of phase portraits in the Poincaré section by hypersurface $y_1 = 0$ for coupled quasiperiodic generators (1) with (3) and $\lambda = 1.4$, $\omega_0 = 2\pi$. a) $\Delta = 5.24$, $M_C = 0.12$; b) $\Delta = 4.96$, $M_C = 0.37$; c) $\Delta = 5.24$, $M_C = 0.39$; d) $\Delta = 4.89$, $M_C = 0.22$; e) $\Delta = 5.61$, $M_C = 0.19$; f) $\Delta = 5.38$, $M_C = 0.26$; g) $\Delta = 5.53$, $M_C = 0.39$ 25

- 4 Zoomed fragment of the chart of Lyapunov exponents (a) and two-dimensional projections of phase portraits in the Poincaré section by hypersurface $y_1 = 0$ for coupled quasiperiodic generators (1) with (3) and $\lambda = 1.4$, $\omega_0 = 2\pi$. b) $\Delta = 5.4$, $M_C = 0.127$; c) $\Delta = 5.5$, $M_C = 0.14$; d) $\Delta = 5.55$, $M_C = 0.146$; e) $\Delta = 5.37$, $M_C = 0.112$ 26

- 5 Two-dimensional projections of phase portraits in the double Poincaré section by hypersurface $y_1 \approx 0$ and $y_2 \approx 0$ for coupled quasiperiodic generators (1) with (3), $\lambda = 1.4$, $\omega_0 = 2\pi$. a) $\Delta = 5.66$, $M_C = 0.123$; b) $\Delta = 5.5$, $M_C = 0.086$; c) $\Delta = 5.341$, $M_C = 0.143$; d) $\Delta = 5.377$, $M_C = 0.145$ 26

- 6 Zoomed fragment of the chart of Lyapunov exponents (a) and two-dimensional projections of phase portraits in the Poincaré section by hypersurface $y_1 = 0$ for coupled quasiperiodic generators (1) with (3) and $\lambda = 1.4$, $\omega_0 = 2\pi$, $\Delta = 5.35$. b) $M_C = 0.133$; c) $M_C = 0.1386$; d) $M_C = 0.1396$; e) $M_C = 0.14$; f) $M_C = 0.14013$; g) $M_C = 0.14014$; h) $M_C = 0.140147$; e) $M_C = 0.140148$ 27

7 Two-dimensional projections of phase portraits in the Poincaré section by hypersurface $y_1 = 0$ for coupled quasiperiodic generators (1) with (3) and $\lambda = 1.4$, $\omega_0 = 2\pi$; a) $\Delta = 5.35$, $M_C = 0.1401481$; b) $\Delta = 5.35$, $M_C = 0.1401483$; c) $\Delta = 5.35$, $M_C = 0.1403$; d) $\Delta = 5.35$, $M_C = 0.142$; e) $\Delta = 5.34$, $M_C = 0.148$ 27

8 Dependence of the largest three Lyapunov exponents on the parameter M_C and its zoomed fragments for (3) and $\lambda = 1.4$, $\omega_0 = 2\pi$, $M_C = 5.3778$. DT^{nm} are bifurcations of torus doubling, n is periodicity window index, m is doubling number, $T_{\frac{1}{2}}^k$ is two-frequency quasiperiodic regime with k -turn invariant curve. 28

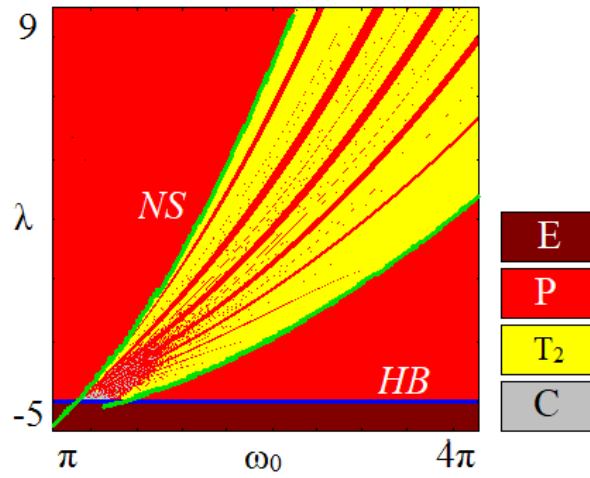


Fig. 1. Chart of Lyapunov exponents and the main bifurcation lines of autonomous generator of quasiperiodic oscillations, system (1) with parameters (3) and $M_C = 0$, $\Delta = 0$. *HB* is line of Andronov-Hopf bifurcation, *NS* is line of Neimark-Sacker bifurcation.

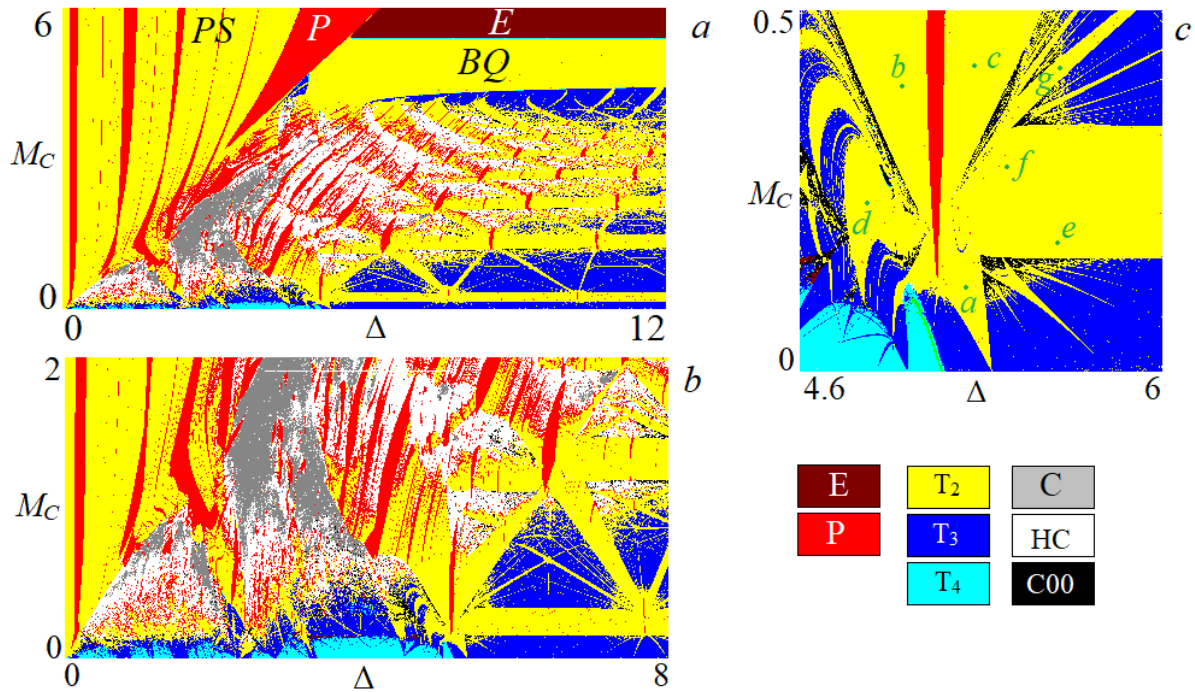


Fig. 2. Chart of Lyapunov exponents and its enlarged fragments for the system of coupled quasiperiodic generators (1) with parameters $\beta = 1/25$, $b = 1$, $\varepsilon = 4$, $k = 0.02$, $\lambda = 1.4$, $\omega_0 = 2\pi$.

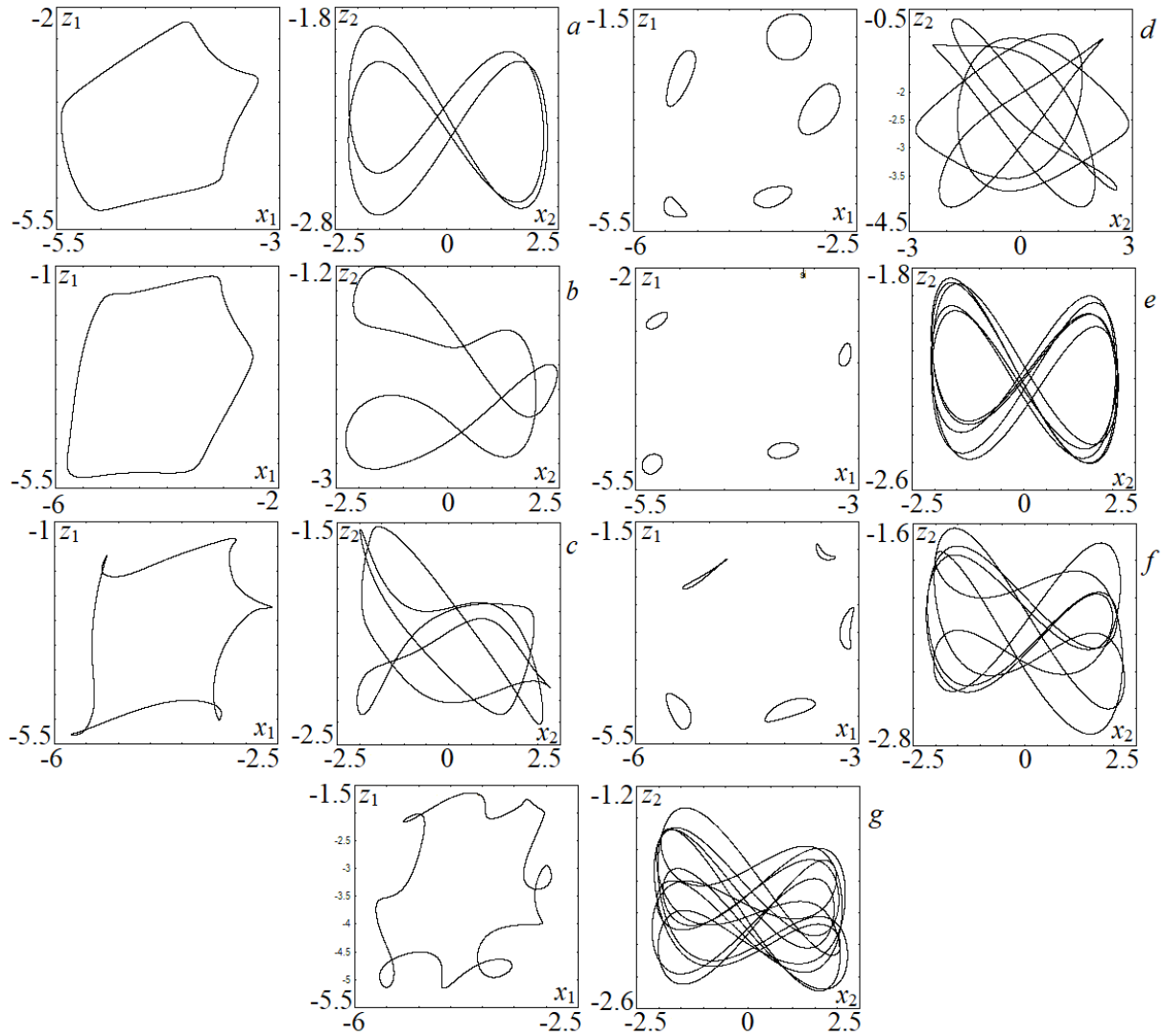


Fig. 3. Two-dimensional projections of phase portraits in the Poincaré section by hypersurface $y_1 = 0$ for coupled quasiperiodic generators (1) with (3) and $\lambda = 1.4$, $\omega_0 = 2\pi$. a) $\Delta = 5.24$, $M_C = 0.12$; b) $\Delta = 4.96$, $M_C = 0.37$; c) $\Delta = 5.24$, $M_C = 0.39$; d) $\Delta = 4.89$, $M_C = 0.22$; e) $\Delta = 5.61$, $M_C = 0.19$; f) $\Delta = 5.38$, $M_C = 0.26$; g) $\Delta = 5.53$, $M_C = 0.39$.

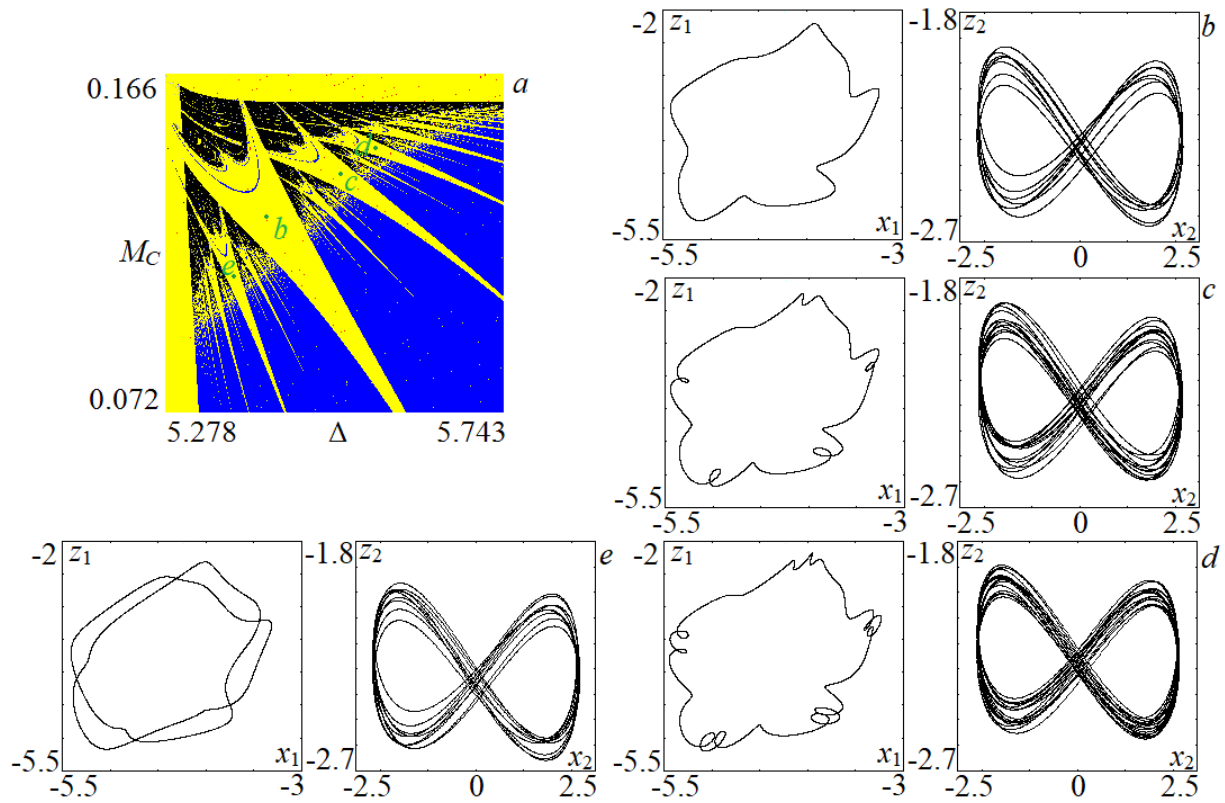


Fig. 4. Zoomed fragment of the chart of Lyapunov exponents (a) and two-dimensional projections of phase portraits in the Poincaré section by hypersurface $y_1 = 0$ for coupled quasiperiodic generators (1) with (3) and $\lambda = 1.4$, $\omega_0 = 2\pi$. b) $\Delta = 5.4$, $M_C = 0.127$; c) $\Delta = 5.5$, $M_C = 0.14$; d) $\Delta = 5.55$, $M_C = 0.146$; e) $\Delta = 5.37$, $M_C = 0.112$.

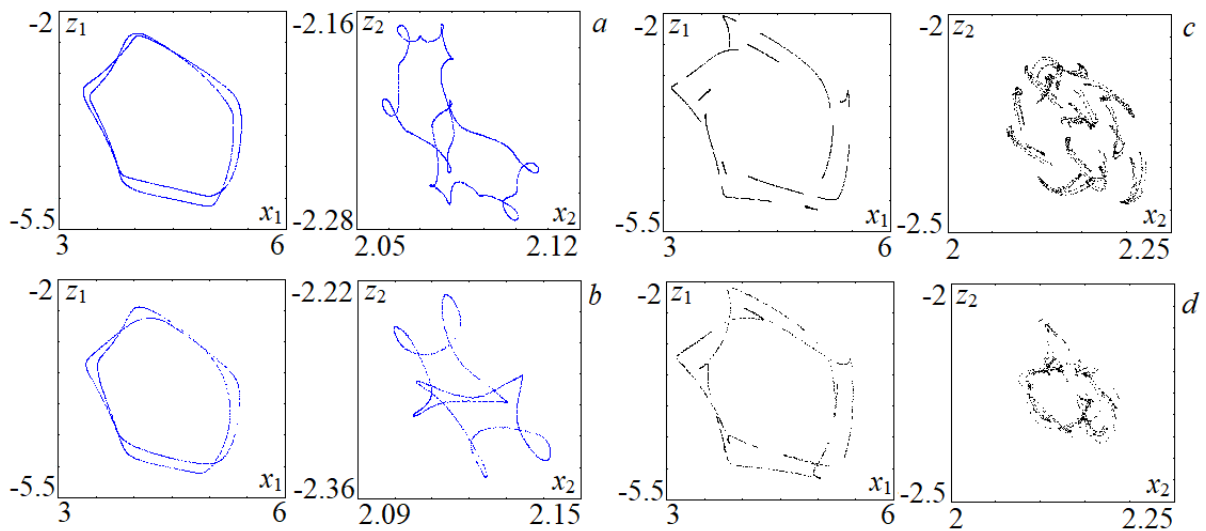


Fig. 5. Two-dimensional projections of phase portraits in the double Poincaré section by hypersurface $y_1 \approx 0$ and $y_2 \approx 0$ for coupled quasiperiodic generators (1) with (3), $\lambda = 1.4$, $\omega_0 = 2\pi$. a) $\Delta = 5.66$, $M_C = 0.123$; b) $\Delta = 5.5$, $M_C = 0.086$; c) $\Delta = 5.341$, $M_C = 0.143$; d) $\Delta = 5.377$, $M_C = 0.145$.

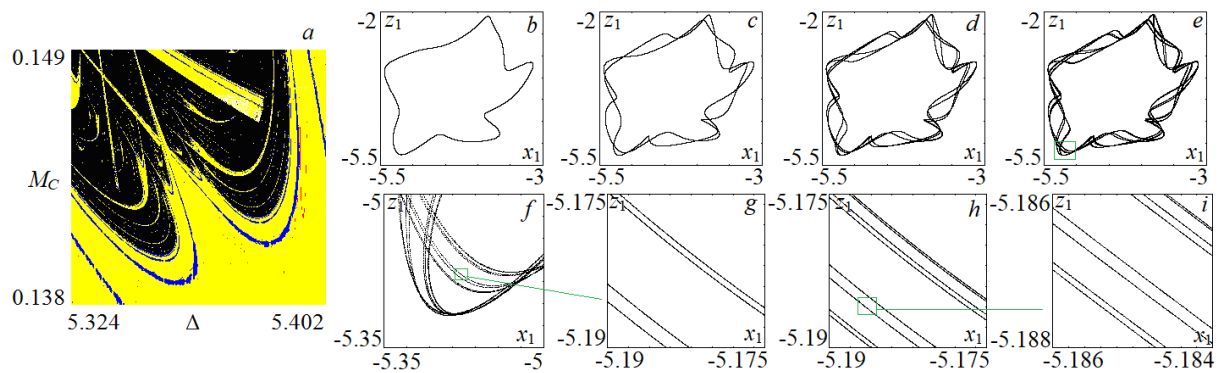


Fig. 6. Zoomed fragment of the chart of Lyapunov exponents (a) and two-dimensional projections of phase portraits in the Poincaré section by hypersurface $y_1 = 0$ for coupled quasiperiodic generators (1) with (3) and $\lambda = 1.4$, $\omega_0 = 2\pi$, $\Delta = 5.35$. b) $M_C = 0.133$; c) $M_C = 0.1386$; d) $M_C = 0.1396$; e) $M_C = 0.14$; f) $M_C = 0.14013$; g) $M_C = 0.14014$; h) $M_C = 0.140147$; i) $M_C = 0.140148$.

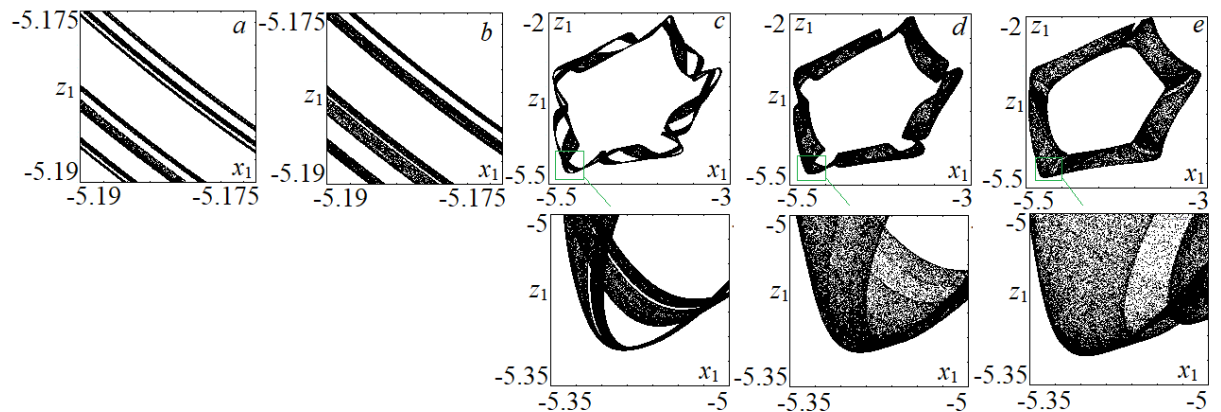


Fig. 7. Two-dimensional projections of phase portraits in the Poincaré section by hypersurface $y_1 = 0$ for coupled quasiperiodic generators (1) with (3) and $\lambda = 1.4$, $\omega_0 = 2\pi$; a) $\Delta = 5.35$, $M_C = 0.1401481$; b) $\Delta = 5.35$, $M_C = 0.1401483$; c) $\Delta = 5.35$, $M_C = 0.1403$; d) $\Delta = 5.35$, $M_C = 0.142$; e) $\Delta = 5.34$, $M_C = 0.148$.

Table 1. Accordance between signature of the Lyapunov exponents spectrum of observed regimes and symbols used for the charts of Lyapunov exponents for 3D system of autonomous quasiperiodic generator

Regime	Signature of the spectrum of Lyapunov exponents	Symbol
stable equilibrium point	$0 > \Lambda_1 > \Lambda_2 > \Lambda_3$	E
periodic	$\Lambda_1 = 0, 0 > \Lambda_2 > \Lambda_3$	P
two-frequency quasiperiodic	$\Lambda_1 = 0, \Lambda_2 = 0, 0 > \Lambda_3$	T ₂
chaotic	$\Lambda_1 > 0, \Lambda_2 = 0, 0 > \Lambda_3$	C

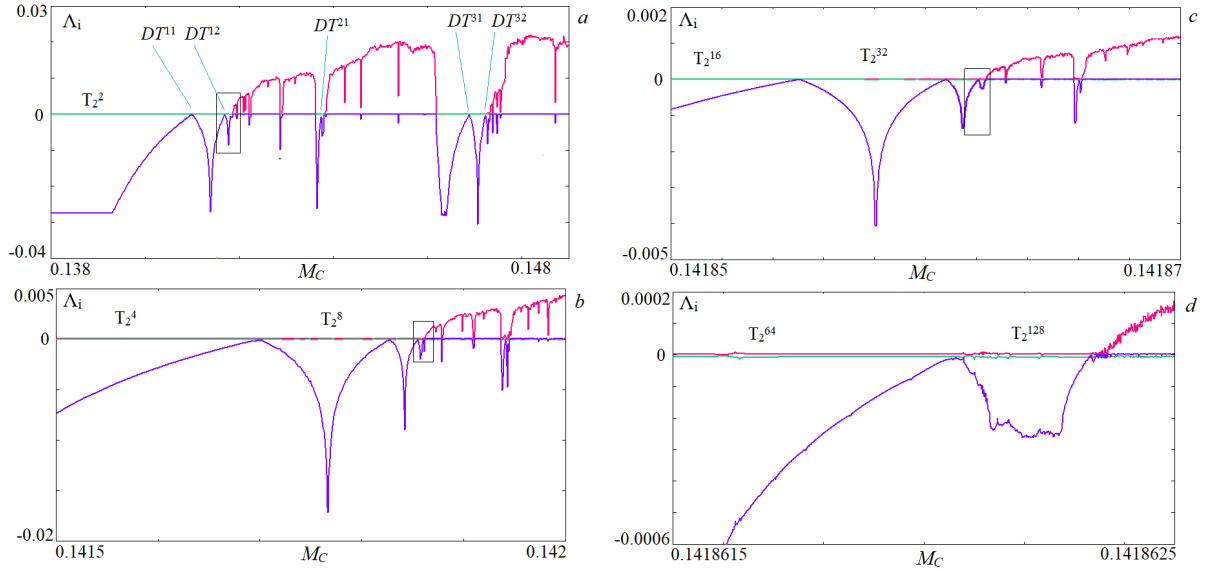


Fig. 8. Dependence of the largest three Lyapunov exponents on the parameter M_C and its zoomed fragments for (3) and $\lambda = 1.4$, $\omega_0 = 2\pi$, $M_C = 5.3778$. DT^{nm} are bifurcations of torus doubling, n is periodicity window index, m is doubling number, T_2^k is two-frequency quasiperiodic regime with k -turn invariant curve.

Table 2. Accordance between signature of the Lyapunov exponents spectrum of observed regimes and symbols used for the charts of Lyapunov exponents for 6D system of coupled generators

Regime	Signature of the spectrum of Lyapunov exponents	Symbol
stable equilibrium point	$0 > \Lambda_1 > \Lambda_2 > \Lambda_3 > \Lambda_4 > \Lambda_5 > \Lambda_6$	E
periodic	$\Lambda_1 = 0, 0 > \Lambda_2 > \Lambda_3 > \Lambda_4 > \Lambda_5 > \Lambda_6$	P
two-frequency quasiperiodic	$\Lambda_1 = 0, \Lambda_2 = 0, 0 > \Lambda_3 > \Lambda_4 > \Lambda_5 > \Lambda_6$	T_2
three-frequency quasiperiodic	$\Lambda_1 = 0, \Lambda_2 = 0, \Lambda_3 = 0, 0 > \Lambda_4 > \Lambda_5 > \Lambda_6$	T_3
four-frequency quasiperiodic	$\Lambda_1 = 0, \Lambda_2 = 0, \Lambda_3 = 0, \Lambda_4 = 0, 0 > \Lambda_5 > \Lambda_6$	T_4
chaotic	$\Lambda_1 > 0, \Lambda_2 = 0, 0 > \Lambda_3 > \Lambda_4 > \Lambda_5 > \Lambda_6$	C
chaotic (hyperchaos)	$\Lambda_1 > \Lambda_2 > 0, \Lambda_3 = 0, 0 > \Lambda_4 > \Lambda_5 > \Lambda_6$	HC
chaotic (with additional zero LE)	$\Lambda_1 > 0, \Lambda_2 = 0, \Lambda_3 = 0, 0 > \Lambda_4 > \Lambda_5 > \Lambda_6$	C00

Table 3. Signature of the spectrum of the Lyapunov exponents for attractors at transition to chaos via three-torus destruction, parameters (3) and $\lambda = 1.4, \omega_0 = 2\pi$

Δ	M_C	Λ_1	Λ_2	Λ_3	Λ_4
5.660	0.123	0.0	0.0	0.0	-0.04623
5.500	0.086	0.0	0.0	0.0	-0.03237
5.341	0.143	0.01390	0.0	0.0	-0.02479
5.377	0.145	0.01865	0.0	0.0	-0.02757

Table 4. Signature of the spectrum of the Lyapunov exponents for attractors at transition to chaos via two-torus doubling bifurcations, parameters (3) and $\lambda = 1.4, \omega_0 = 2\pi$

Δ	M_C	Λ_1	Λ_2	Λ_3	Λ_4
5.35	0.1401481	0.00012	0.0	0.0	-0.02523
5.35	0.1401483	0.00017	0.0	0.0	-0.02519
5.35	0.1403000	0.00310	0.0	0.0	-0.02525
5.35	0.1420000	0.00837	0.0	0.0	-0.02538
5.35	0.1480000	0.01847	0.0	0.0	-0.02507